

Genomic variability and alternative splicing generate multiple PML/RAR α transcripts that encode aberrant PML proteins and PML/RAR α isoforms in acute promyelocytic leukaemia

P.P.Pandolfi, M.Alcalay, M.Fagioli, D.Zangrilli, A.Mencarelli, D.Diverio¹, A.Biondi², F.Lo Coco¹, A.Rambaldi³, F.Grignani, C.Rochette-Egly⁴, M.-P.Gaube⁴, P.Chambon⁴ and P.G.Pelicci

Istituto Clinica Medica I, University of Perugia, Policlinico Monteluce, 06100 Perugia, ¹Dipartimento di Biopatologia, Divisione di Ematologia, I University of Rome, 00161 Rome, ²Clinica Pediatrica, University of Milan, Ospedale S.Gerardo, 20052 Monza, ³Divisione di Ematologia, Ospedali Riuniti Bergamo e Istituto Ricerche Farmacologiche 'M.Negri', 24100 Bergamo, Italy and ⁴Laboratoire de Génétique Moléculaire des Eucaryotes du CNRS, Unité de Biologie Moléculaire et de Génie Génétique de l'INSERM, Institut de Chimie Biologique, Faculté de Médecine, 67085 Strasbourg, Cedex, France

Communicated by E.Boncinelli

The acute promyelocytic leukaemia (APL) 15;17 translocation generates a PML/RAR α chimeric gene which is transcribed as a fusion PML/RAR α mRNA. Molecular studies on a large series of APLs revealed great heterogeneity of the PML/RAR α transcripts due to: (i) variable breaking of chromosome 15 within three PML breakpoint cluster regions (*bcr1*, *bcr2* and *bcr3*), (ii) alternative splittings of the PML portion and (iii) alternative usage of two RAR α polyadenylation sites. Nucleotide sequence analysis predicted two types of proteins: multiple PML/RAR α and aberrant PML. The PML/RAR α proteins varied among *bcr1*, 2 and 3 APL cases and within single cases. The fusion proteins contained variable portions of the PML N terminus joined to the B–F RAR α domains; the only PML region retained was the putative DNA binding domain. The aberrant PML proteins lacked the C terminus, which had been replaced by from two to ten amino acid residues from the RAR α sequence. Multiple PML/RAR α isoforms and aberrant PML proteins were found to coexist in all APLs. These findings indicate that two potential oncogenic proteins are generated by the t(15;17) and suggest that the PML activation pathway is altered in APLs.

Key words: aberrant PML/acute promyelocytic leukaemia/alternative splicing/chromosome translocation/PML/RAR α

Introduction

The study of chromosomal translocations associated with haemopoietic tumours has led to the identification of new genes involved in neoplastic transformation and to a better understanding of the pathogenesis of these tumours. Examples are the recombination of the *bcr* and *abl* genes in the t(9;22) of chronic myeloid leukaemia and the *myc* and immunoglobulin genes in the t(8;14) of Burkitt lymphoma (Sawyers *et al.*, 1991).

Three groups, including ours, have demonstrated that the two genes involved in the t(15;17) of acute promyelocytic

leukaemia (APL), a subtype of acute myeloid leukaemia (AML), are PML (also designated *myl*) on chromosome 15 and retinoic acid receptor α (RAR α) on 17 (Borrow *et al.*, 1990; de Thé *et al.*, 1990; Longo *et al.*, 1990a,b; Alcalay *et al.*, 1981).

The t(15;17) is detected cytogenetically in 70% and molecularly in 100% of APL cases; it is often the only karyotypic alteration and has never been detected in other malignancies (Mitelman, 1988; Biondi *et al.*, 1991). These observations are reasonable evidence that the t(15;17) is directly involved in the pathogenesis of APLs.

Chimeric RAR α /PML and PML/RAR α genes are formed as the consequence of the reciprocal translocation between the PML and RAR α loci. The chimeric PML/RAR α gene is expressed as a fusion mRNA (de Thé *et al.*, 1990; Longo *et al.*, 1990b). We and others have recently isolated the PML/RAR α cDNA and demonstrated that it encodes a fusion protein that contains large portions of both the PML and RAR α proteins (de Thé *et al.*, 1991; Kakizuka *et al.*, 1991; Pandolfi *et al.*, 1991). The role of this fusion protein in the pathogenesis of APL, and the importance of the PML or RAR α abnormalities, remain unknown.

Retinoic acid (RA) induces terminal differentiation of myeloid precursors (Breitman *et al.*, 1980). The effect is mediated by RAR α (Collins *et al.*, 1980). An abnormal RAR α protein could, therefore, contribute to the leukaemic phenotype by blocking further differentiation of promyelocytes. This explanation contrasts with the finding that RA induces terminal differentiation of APL blasts both *in vitro* and *in vivo* (Huang *et al.*, 1988; Castaigne *et al.*, 1990; Chomienne *et al.*, 1990; Lo Coco *et al.*, 1991; Warrel *et al.*, 1991). Although it is obvious that the PML abnormality could also underlie promyelocytic leukaemogenesis, we know far too little about PML to advance any hypothesis on its putative role in APLs.

RAR α is one of the nuclear receptors that function to regulate gene expression in response to the binding of RA (Giguere *et al.*, 1987; Petkovich *et al.*, 1987). The capacity of PML/RAR α to act as a retinoid-inducible transcription factor has been tested by assessing its ability to regulate the expression of specific RA-responsive reporter genes. We have previously reported that PML/RAR α acts as a transcription factor with both RA-independent repressor and RA-dependent activator functions (Pandolfi *et al.*, 1991). Others have obtained similar results using different reporter genes and target cells (de Thé *et al.*, 1991; Kakizuka *et al.*, 1991). However, de Thé *et al.* (1991) also observed RA-dependent repressor function and Kakizuka *et al.* (1991) observed constitutive activator functions. It therefore seems that PML/RAR α has both promoter and cell-type specificities, but the effect it exerts on target genes involved in myeloid differentiation remains obscure.

There is evidence that the PML/RAR α genes and fusion transcripts are heterogeneous: (i) PML genomic DNA probes detect rearrangements in only 70% of APL cases (Biondi

et al., 1991); (ii) three RAR α aberrant transcripts of 4.4, 4.0 and 3.5 kb have been identified in APLs (Longo *et al.*, 1990b); (iii) four PML/RAR α isoforms that differ in their PML portion have been reported (de Thé *et al.*, 1991; Kakizuka *et al.*, 1991; Pandolfi *et al.*, 1991). Because PML and RAR α are both modular proteins, the identification of the functional domains that are consistently present in the PML/RAR α fusion protein should help to define its functional properties. The RAR α protein can be divided into six regions, A–F, on the basis of sequence homology with other members of the nuclear receptor superfamily (Evans, 1988; Green and Chambon, 1988; Beato, 1989). The C region is a DNA binding domain, the E region contains domains for ligand binding, nuclear localization, receptor dimerization and transcriptional activation and the A/B region has transcriptional activation functions with cell-type and promoter specificity. The PML protein contains a cysteine-rich motif (de Thé *et al.*, 1991; Kakizuka *et al.*, 1991) which resembles the zinc finger DNA binding domain common to several classes of transcriptional factors (Evans and Hollenberg, 1988; Berg, 1990; Freemont *et al.*, 1991) and an α -helical domain that includes a segment with homology to the leucine zipper region of the *fos* family (Cohen and Curran, 1988; Zerial *et al.*, 1989).

Our present analysis of PML/RAR α genes and the resulting fusion transcripts and proteins in a large series of APL cases shows that the breakpoint within the PML locus is variably situated, the PML/RAR α transcripts differ and, due to alternative splicing in the PML portion, multiple PML/RAR α isoforms coexist in single cases. The predicted PML/RAR α proteins all conserve the PML cysteine-rich domain and the RAR α B–F domains. PML/RAR α transcripts that code for aberrant PML proteins were also identified in all APL cases examined.

These data provide a detailed blueprint of the molecular architecture of the t(15;17) and support the hypothesis that abnormal PML proteins are involved in the promyelocytic leukaemogenesis.

Results

The APL chromosome 17 breakpoint is consistently located within RAR α intron 2

To determine the localization of the chromosome 17 breakpoint, DNAs from 43 APL cases were studied in Southern blot experiments using combinations of restriction enzymes and genomic RAR α probes which explore ~25 kb of the RAR α locus 5' portion (Figure 1A). The results of nine representative cases will be described below (Figure 1B).

Digestion with *Hind*III and hybridization with H18 and HB probes revealed rearrangements of the 19 kb *Hind*III fragment in six of nine cases. Two different rearranged fragments, the two translocation reciprocals were detected in cases 8, 13 and 20. The single H18 or HB *Hind*III rearrangements in cases 11, 18 and 27 could be the result of comigration of rearranged bands with germline fragments.

Cases 28, 10 and 22, which were germline upon *Hind*III digestion and hybridization to both H18 and HB probes, displayed rearrangements in the 6.6 kb *Eco*RI fragment explored by the H18 probe. Double digestion with *Pst*I and *Eco*RI restriction enzymes and hybridization with the H18 probe mapped the chromosome 17 breakpoint to RAR α

intron 2 in cases 10 and 22. The breakpoint site in case 28 could not be precisely mapped by Southern blot analysis; however, cloning of both translocation reciprocals from this case demonstrated that the breakpoint lay within RAR α intron 2 180 bp 5' to the *Pst*I site (data not shown). Cases 8, 11 and 18 had rearrangements in the X5' hybridizing 12 kb *Eco*RI fragment, which is entirely contained within RAR α intron 2. The remaining cases (13, 20 and 27) displayed rearrangements of the HB hybridizing 5.5 kb *Eco*RI fragment. Since this fragment contains RAR α exons 3 and 4, the translocation breakpoint was further mapped in these cases. All three were rearranged in the K5' hybridizing 3 kb *Kpn*I–*Eco*RI fragment contained within intron 2.

Genomic cloning and Southern blotting data led to the conclusion that the chromosome 17 breakpoint was located within intron 2 in all 43 APL cases analysed. Therefore, it would seem that the PML/RAR α gene consistently retains the RAR α exon 3 and 3' sequences which code for domains B–F.

Isolation of the PML locus

A human embryo lung fibroblast genomic library was screened with the M1 PML cDNA probe previously reported (Pandolfi *et al.*, 1991). Positive clones were analysed by restriction enzyme mapping and hybridization to probes representative of different portions of the PML cDNA and the exon/intron boundaries sequenced. The exon/intron organization of the PML locus is shown in Figure 2A (partial nucleotide sequence data are given in Figures 3, 4 and 6). The PML locus has seven exons which span a minimum of 30 kb. The PML coding region is contained within exons 1–7.

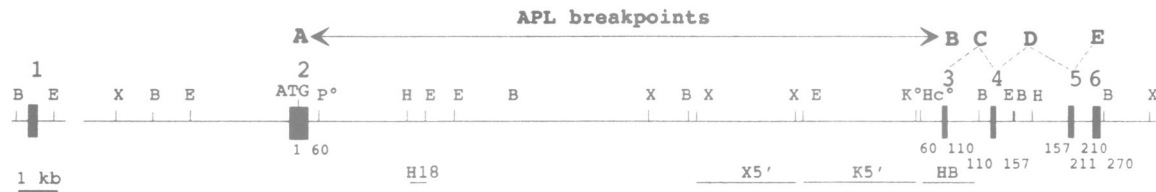
The PML protein contains an N-terminal proline-rich motif, a cysteine-rich motif, an α -helical domain, a leucine zipper homologous region and a serine-rich motif. The cysteine-rich motif is divided into three clusters (de Thé *et al.*, 1991; Kakizuka *et al.*, 1991). The proline-rich motif is contained within exon 1; the first and second cysteine-rich clusters are within exon 2; the third spans exons 2 and 3; the α -helical domain is split among exons 3–6; the leucine zipper homologous region is contained within exon 3 and the serine-rich motif within exon 6 (Figure 2A).

The APL chromosome 15 breakpoint is variably located within three breakpoint cluster regions (*bcr*1, 2 and 3)

The chromosome 15 breakpoint was mapped within the PML locus in the 43 APL cases previously analysed for the 17 breakpoint (Figure 2A). The results of 11 cases will be described below (Figure 2B).

In a previously analysed case the chromosome 15 breakpoint was located within PML intron 6 (Alcalay *et al.*, 1991); this region was therefore investigated first in all cases. DNAs were digested with *Eco*RI and *Hind*III and hybridized to the RH15 DNA probe. Five cases (18, 37, 40, 35 and 36) displayed rearrangements with both enzymes, indicating that the breakpoint is located within the 2.8 kb *Hind*III–*Eco*RI fragment containing exons 5 and 6. In all five cases the 5.5 kb *Kpn*I fragment detected by probe RH15 was rearranged. Double digestion with *Bgl*I and *Eco*RI and sequential hybridizations with the BG1 and BG2 probes mapped the chromosome 15 breakpoint to PML intron 6 in

A

RAR- α 

B

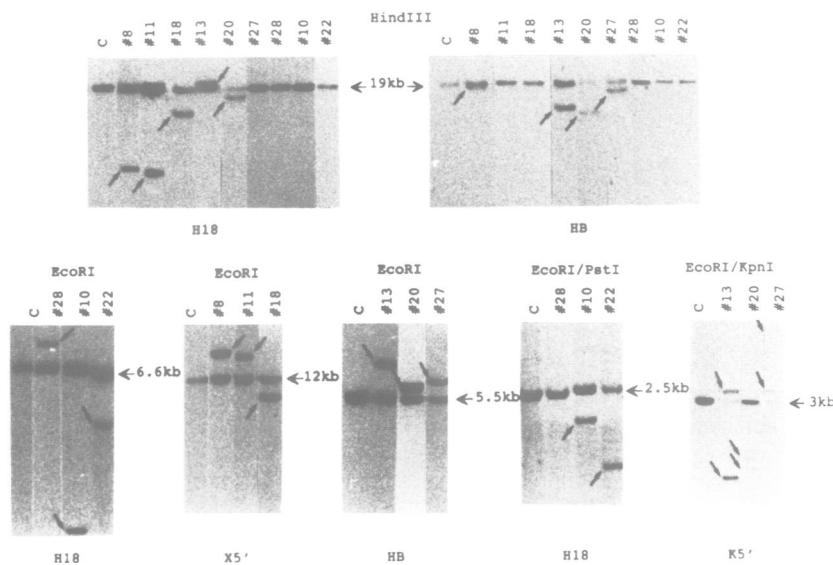


Fig. 1. Mapping of chromosome 17 breakpoints in APLs. (A) Limited restriction enzyme map of the RAR α locus 5' portion (Brand *et al.*, 1990; Alcalay *et al.*, 1991). Black boxes indicate RAR α exons (exon numbers are given above the map). Exon 2 contains the translation initiation codon (ATG); positions of the RAR α residues are given below the corresponding coding exons. The exons encoding the RAR α A–E functional domains are indicated (regions encoded by more than one exon are shown by broken lines). Domain E is encoded by exon 6 and the more 3' exons. The RAR α DNA probes used in this study are indicated as solid lines below the map. B, *Bam*HI; E, *Eco*RI; H, *Hind*III; X, *Xba*I; K, *Kpn*I; P, *Pst*I; Hc, *Hinc*II. ° indicates that only relevant sites are shown. The arrowed line above the map shows the region of APL breakpoints. (B) Southern blot analysis of nine representative APL cases. APL DNAs (APL case numbers are given above each blot) and human placenta DNA (C) were digested with the restriction enzyme(s) indicated above the blots and hybridized to the probes indicated below the blots. Molecular weights of germline hybridizing fragments are given. Rearranged fragments are arrowed.

only three cases (18, 37 and 35), indicating that there are two breakpoint cluster regions (*bcrs*), one in intron 6 (*bcr1*), the other in the 1.3 kb *KpnI*–*BglI* fragment that contains exon 5, intron 5 and exon 6 (*bcr2*).

Cases 38 and 41 had rearrangements of the 9 kb RH15 hybridizing *Hind*III fragment, but not of the 7 kb RH15 *Eco*RI fragment. Double digestion with *Eco*RI and *Bcl*I restriction enzymes and hybridization with the MLU probe mapped the chromosome 15 breakpoint within intron 6 in both cases (*bcr1*).

Probe RH15 detected no *Eco*RI or *Hind*III rearranged fragments in the remaining four cases (29, 33, 30 and 34; data not shown). However, hybridization of *Hind*III (Figure 2B) and *Eco*RI (not shown) digests with the LAEP probe revealed rearrangements in all cases. The 4 kb *Hind*III–*Eco*RI fragment which spans the region from within intron 2 to the 5' end of intron 4 is yet another breakpoint cluster region (*bcr3*).

As there are no appropriate restriction enzyme sites within

the PML locus that would allow finer Southern blot mapping of breakpoints, APL cases representative of each *bcr* were analysed by cloning the PML/RAR α chimeric gene. The restriction enzyme maps of the three representative PML/RAR α loci are shown in Figure 2A. The chromosome 15 breakpoint was located within intron 6 in case 26 (*bcr1*), within exon 6 in case 29 (*bcr2*) and within intron 3 in case 8 (*bcr3*).

***bcr1*, *bcr2* and *bcr3* PML/RAR α mRNA junctions differ**

The PML/RAR α mRNA junctions from a large series of APLs representative of the three different *bcrs* were PCR amplified and the nucleotide sequences determined. Primer M2 derived from the PML exon 5 and primer R8 from RAR α exon 3 were used for amplification of *bcr1* and *bcr2* PML/RAR α mRNA junctions. Primer M4 derived from PML exon 3 and primer R8 were used for amplification of *bcr3* PML/RAR α mRNA junctions (Figures 3 and 4).

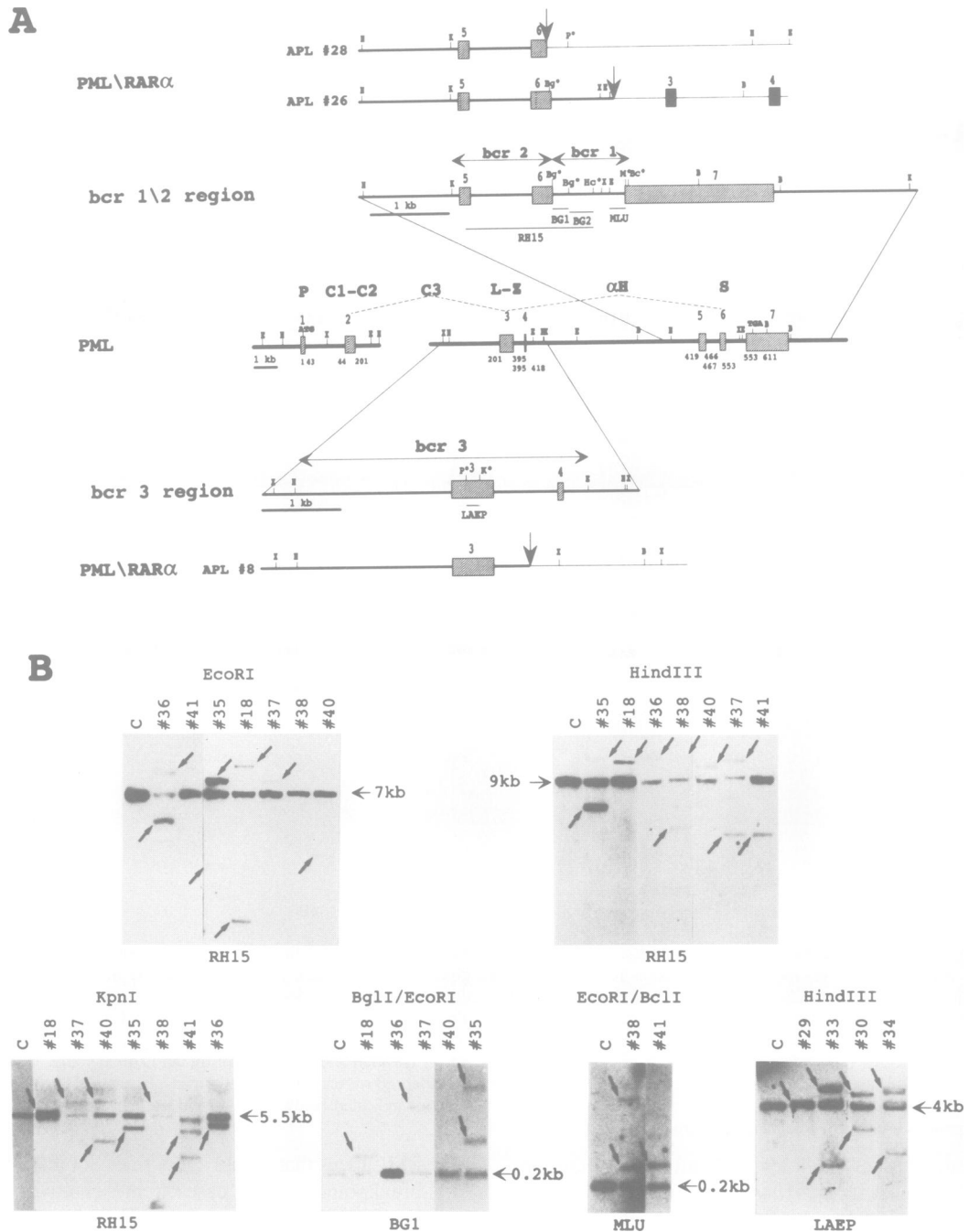


Fig. 2. Mapping of chromosome 15 breakpoints in APLs. (A) Limited restriction enzyme map of the normal PML locus and of the PML/RAR α fusion genes from three APL cases. A limited map of the PML locus is shown in the middle, as indicated. Hatched boxes indicate PML exons. Exon numbers are given above the map (the numbering is temporary since the cap site has not been mapped). There is a gap within the PML locus map because the isolated PML genomic clones did not overlap. Positions of the PML amino acid residues are given below the corresponding coding exons. The regions coding for the PML proline-rich motif (P), the three cysteine-rich clusters (C1, C2 and C3), the α -helical domain (α H), the leucine zipper homologous region (L-Z) and the serine-rich motif (S) are indicated above the map (regions encoded by more than one exon are shown by broken lines). The regions involved in chromosome 15 breakpoints are enlarged: *bcr1* and *bcr2* are given above and *bcr3* below the map. The limits of *bcrs*, as determined by Southern blotting, are indicated by the double arrowed lines. The PML/RAR α fusion genes from *bcr1* APL case 26 and *bcr2* case 28 are given above. The PML/RAR α fusion gene from the *bcr3* APL case 8 is shown below. RAR α exons are shown as black boxes. Vertical arrows indicate PML/RAR α genomic junctions. PML DNA probes used in this study are indicated as solid bars below the maps. B, BamHI; E, EcoRI; H, HindIII; X, XbaI; K, KpnI; Bg, BglI; Bc, BclI; P, PstI; M, MluI; Hc, HincII. The \circ indicates that only relevant sites are shown. (B) Southern blot analysis of 11 representative APL cases. APL DNAs (patient numbers are given above the blots) and human placenta DNA (C) were digested with the restriction enzyme(s) indicated above the blots and hybridized to the probes indicated below the blots. Molecular weights of germline hybridizing fragments are given. Rearranged fragments are arrowed.

A 326 bp amplification product was obtained in 16 *bcr1* APL cases (see Figure 3C for eight representative cases). The nucleotide sequence, which was analysed in three cases

(Figure 3A), revealed that PML exon 6 and RAR α exon 3 were continuous and joined by a correct splicing event. The PML/RAR α junction generated a GCC triplet that codes for

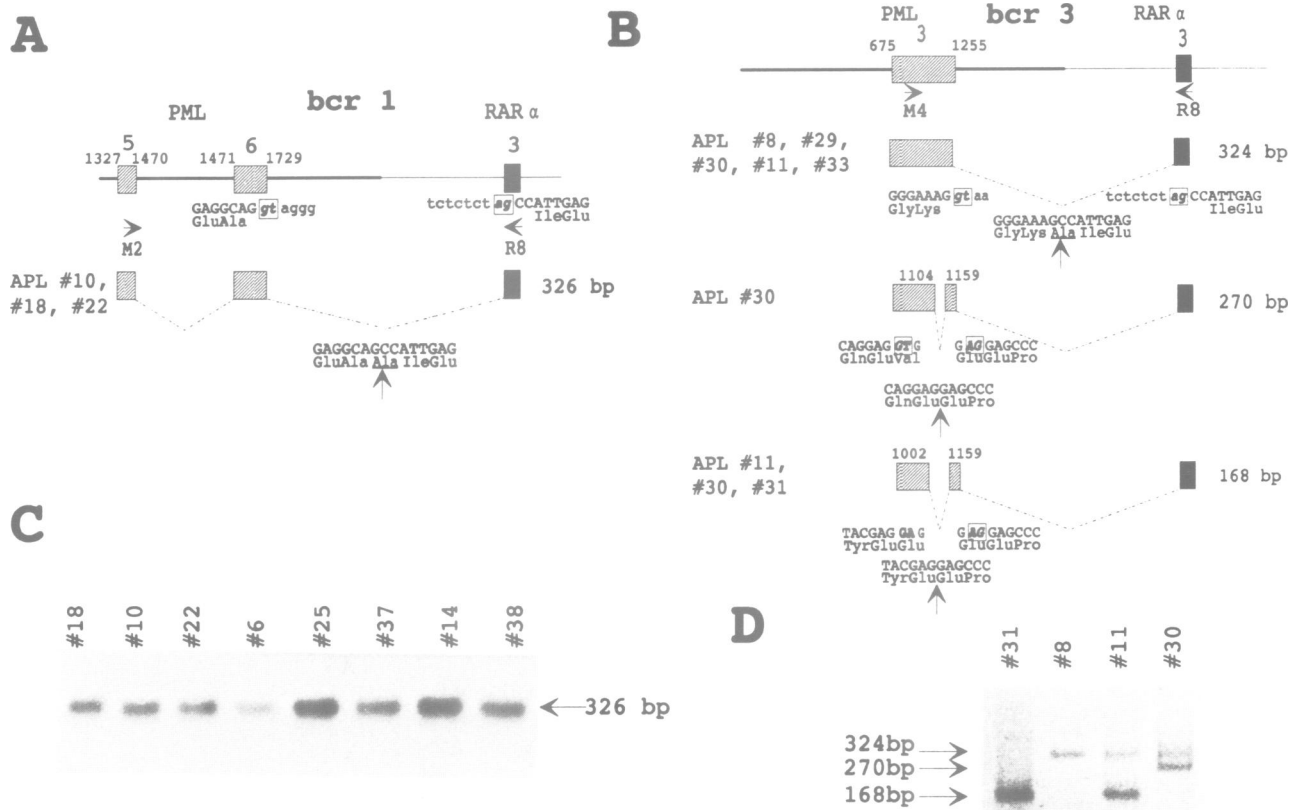


Fig. 3. PML/RAR α mRNA junctions from *bcr1* and *bcr3* APLs. (**A** and **B**) **Upper diagram:** schematic representation of a PML/RAR α *bcr1* (**A**) and *bcr3* (**B**) genomic junctions. Exon numbers and symbols are the same as in Figures 1 and 2. Nucleotide positions, derived from the reported PML cDNA sequence (Pandolfi *et al.*, 1991), are shown above the extremities of the corresponding PML exons. The nucleotide sequences of the PML donor and the RAR α acceptor involved in the PML/RAR α mRNA junction are indicated below the map. The exon and intron sequences are shown in upper and lower cases and the predicted amino acid residues given below. The *gt* and *ag* splicing consensus dinucleotides are in bold and boxed. Note that the 156 bp retained intron has a non-canonical donor site (bold GA dinucleotide in the sequence below the 168 bp fragment diagram). The position and orientation of the M2, M4 and R8 primers are indicated by arrowheads. **Lower diagram:** schematic representation of the exon assembly predicted from the nucleotide sequence of the 326 bp *bcr1* PML/RAR α mRNA PCR amplification product from the indicated APL cases (**A**) and of the 324, 270 and 168 *bcr3* PML/RAR α mRNA PCR amplification products from the indicated APL cases (**B**) (splicing events are shown by the zig-zag broken line). The sequence of the PML/RAR α mRNA junctions and predicted proteins is shown below the broken lines. The arrows indicate the *bcr1* and *bcr3* junctions and exon 3 internal splicings; the non-homologous alanine residue found at both junctions is underlined. (**C** and **D**) PCR blot of eight representative *bcr1* (**C**) and four representative *bcr3* (**D**) APL cases (case numbers are shown above each blot). PCR amplified fragments were hybridized to 20mer oligonucleotides from PML exon 5 (**C**) or exon 3 (**D**) (see Materials and methods).

an alanine residue not found in either the corresponding PML or RAR α sequences.

PCR amplification of the PML/RAR α mRNA junctions from three *bcr2* APL cases yielded four fragments of different lengths: two of 272 bp and 168 bp from case 13; a single 290 bp from case 28 and a single 203 bp from case 32 (Figure 4C). Nucleotide sequence of these fragments revealed that variable portions of PML exon 6 were joined to RAR α exon 3 in each case: exon 6 sequences up to nucleotide 1675 of the reported PML cDNA sequence (Pandolfi *et al.*, 1991) in the 272 bp fragment, up to 1571 in the 168 bp, up to 1577 in the 203 bp and up to 1668 in the 290 bp (Figure 4A and B).

The PML and RAR α sequences were directly joined in both the 272 bp and 168 bp products of case 13 (Figure 4A). The joining of PML and RAR α in the 272 bp product generated a single non-homologous threonine residue and maintained the longest RAR α open reading frame (ORF). The corresponding fusion transcript would therefore be

expected to encode a PML/RAR α fusion protein. The PML and RAR α ORFs were not aligned in the 168 bp product from the same APL case (13) and a TGA termination codon was situated 4 bp 3' to the PML/RAR α junction (Figure 4A). The fusion transcript should therefore encode an aberrant PML protein with two C-terminal amino acid residues (serine and histidine) not homologous to either PML or RAR α (Figure 4A).

The PML and RAR α sequences were interrupted by 25 and 29 nucleotides respectively in the APL case 28 290 bp and in the APL case 32 203 bp fragments (Figure 4A and B). These intervening nucleotides lacked homology with either the PML or RAR α cDNA sequences and did not alter the correct alignment of the longest PML and RAR α ORFs. The resulting PML/RAR α proteins contained residues not homologous with either PML or RAR α at the junction: nine new residues in the fusion protein of cases 28 and 10 in the fusion protein of case 32 (Figure 4A and B).

To determine the origin of the non-homologous PML/

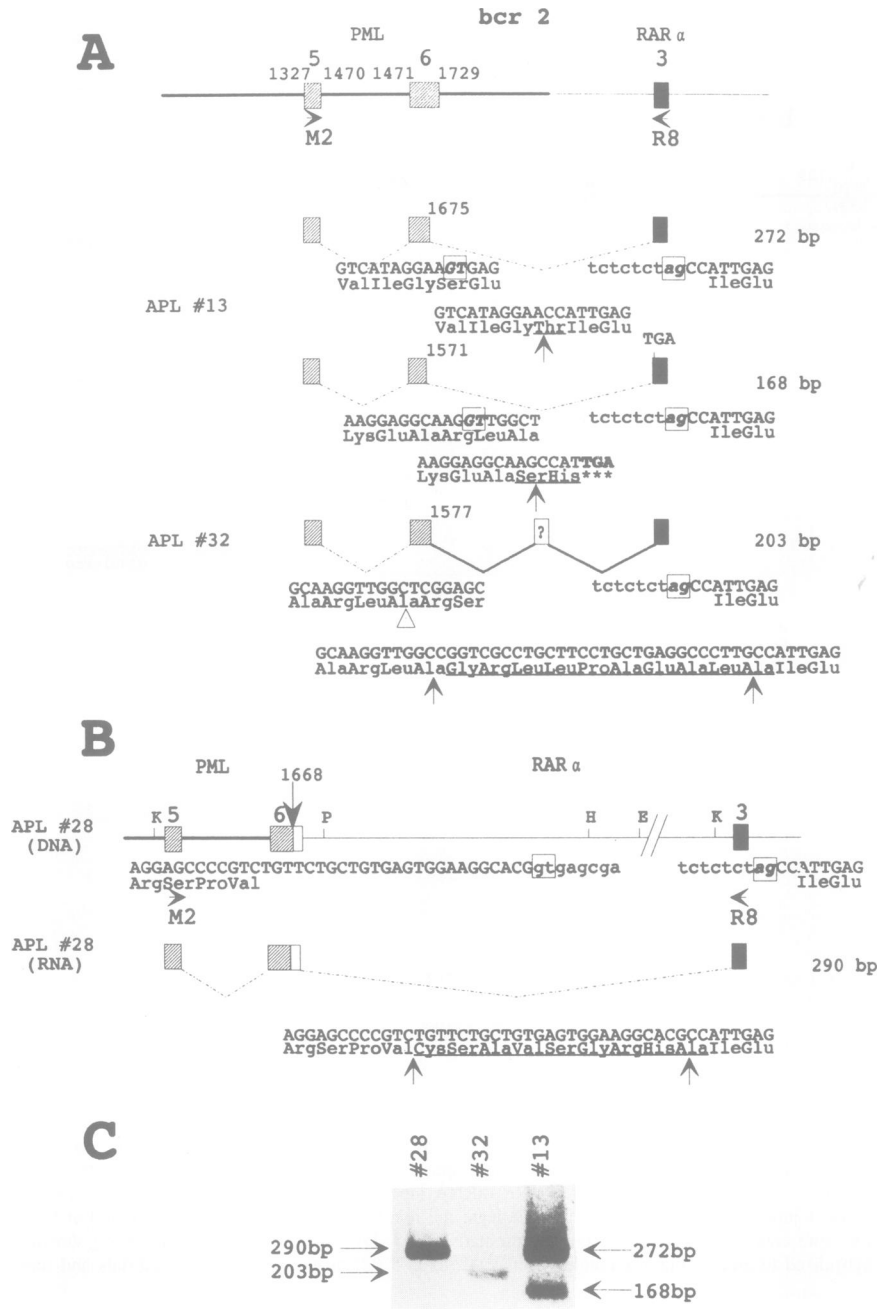


Fig. 4. PML/RARα mRNA junctions from *bcr2* APL cases. **(A) Upper diagram:** schematic representation of a PML/RARα *bcr1* genomic junction. Exon numbers and symbols are the same as in Figures 1 and 2. The position and orientation of the M2 and R8 primers are indicated by arrowheads. **Middle diagrams:** schematic representation of the exon assembly predicted from the nucleotide sequence of the 272 and 168 bp *bcr2* PML/RARα mRNA PCR amplification products from APL case 13. The junctions are arrowed and junctional non-homologous residues are underlined. An in-frame termination codon (★★★) was found 4 bp 3' to the junction in the 168 bp product from case 13. **Lower diagram:** schematic representation of the exon assembly predicted from the nucleotide sequence of the 203 bp *bcr2* PML/RARα mRNA PCR amplification product from APL case 32. The triangle signals the site of divergence between PML/RARα and PML exon 6 sequences (no splicing consensus sequence was found near this site). The two arrows define the limits of the non-homologous junctional sequence, which is indicated by a question mark in the upper diagram. The solid zig-zag lines that connect this non-homologous junctional sequence to the PML exon 6 and the RARα exon 3 mark the undefined mechanism of joining. **(B)** Partial restriction enzyme map of the PML/RARα gene from APL case 28 (DNA; upper diagram) and schematic representation of the exon assembly predicted from the nucleotide sequence of the PML/RARα mRNA PCR 290 bp amplification product from the same APL case (RNA; lower diagram). A portion of RARα intron 2 was found at the PML/RARα junction and is bordered by two arrows in the PML/RARα mRNA junction sequence reported below the lower diagram. The same sequence is indicated as a white box adjacent to PML exon 6 in the genomic PML/RARα map (upper diagram). Nucleotide sequences of the PML/RARα genomic junction and of the RARα exon 3 5' border are given below the genomic map. **(C)** PCR blot of the three *bcr2* APL cases of panels (A) and (B) (case numbers are shown above each blot). PCR amplified fragments were hybridized to a 20mer oligonucleotide from PML exon 5 (see Materials and methods).

RARα junctional nucleotides, the PML/RARα genomic locus of case 28 was isolated, the breakpoint sequenced (Figure 4B) and compared with the sequences of the PML

and RARα mRNA junction from the same case and the corresponding normal PML and RARα genomic segments (not shown). The chromosome 15 breakpoint was located

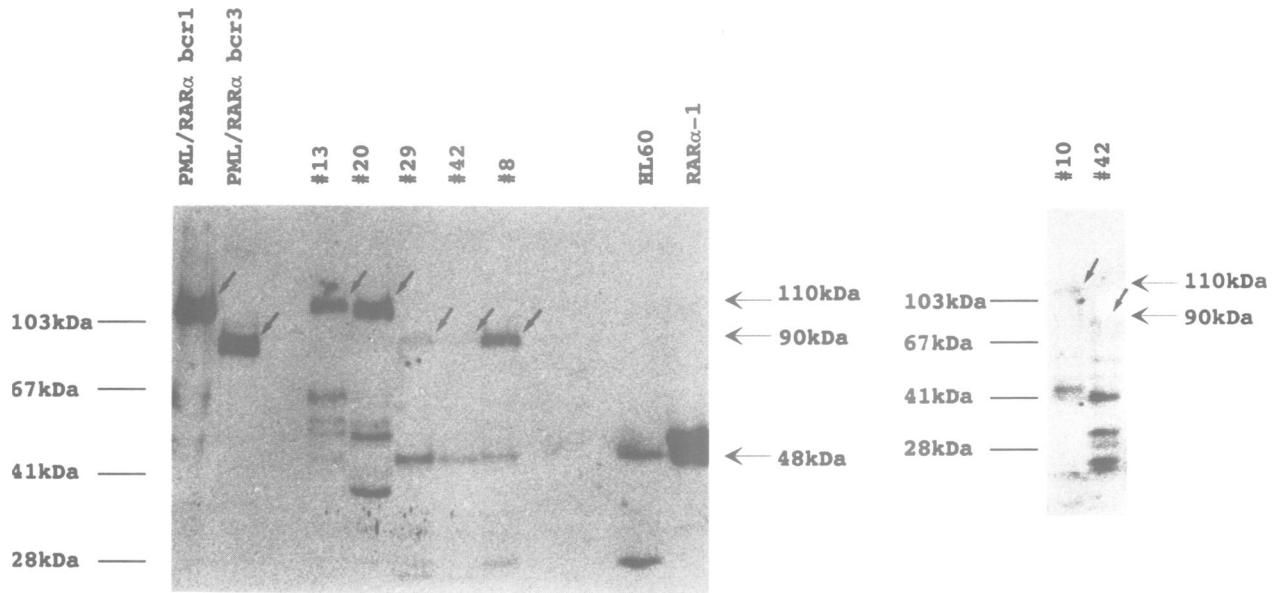


Fig. 5. Western blot analysis of whole cell extracts of APL cells with an anti-RAR α Ab. Whole cell extracts from the indicated cell samples were separated by electrophoresis on a 10% SDS-acrylamide gel and analysed by Western blotting with an Ab directed against the RAR α F domain [RP α (F); see Materials and methods]. PML/RAR α bcr1, PML/RAR α bcr3 and RAR α -1 correspond to COS-1 cells transiently transfected with *bcr1* PML/RAR α , *bcr2* PML/RAR α or RAR α -1 cDNAs. #13 and #20 correspond to *bcr2* APLs; #29, #42 and #8 to *bcr3* APLs; and #10 to a *bcr1* APL. Molecular weight markers are given on the left of each panel. The PML/RAR α bands are arrowed. The approximate molecular weight of *bcr1/2* and *bcr3*, PML/RAR α and RAR α bands is indicated on the right of each panel. The slight migration difference of the 110 kDa band of cases 13 and 20 was not seen in other blots.

within PML exon 6 (position 1668) and the non-homologous 25 nucleotides of the PML/RAR α mRNA junction were derived from the RAR α intron 2 segment located 3' to the breakpoint. A GTGAG cryptic donor was present in RAR α intron 2 immediately 3' to the non-homologous 25 bp fragment. The PML/RAR α junction was therefore formed by the splicing of the truncated PML exon 6 to RAR α exon 3 via the RAR α intron 2 donor consensus and the RAR α exon 3 acceptor.

PCR amplification of the PML/RAR α junction from 15 *bcr3* APL mRNAs identified three variously combined products of 324, 270 and 168 bp (see Figure 3D for four representative cases). All the PCR products visible in the PCR blot of Figure 3D were cloned. Although only the 324 bp and the 270 bp fragments were seen in the PCR blot of case 30, all three fragments were cloned from this case. Nucleotide sequence analysis (Figure 3B) demonstrated that the PML/RAR α junction was always formed by PML exon 3 and RAR α exon 3. As in *bcr1* and *bcr2* cases, the *bcr3* PML/RAR α junction corresponded to an amino acid residue (alanine) that originated from neither PML nor RAR α . The different sizes of the three fragments were due to the splicing out of 54 and 156 bp of PML exon 3 sequences in the 270 and 168 bp products respectively. The 54 bp excised exon sequence was bordered by splicing donor and acceptor in PML exon 3 (Figure 3B). The 156 bp excised exon 3 sequence was bordered by the same donor, but had no acceptor consensus sequence (Jackson, 1991). Therefore, it seems that PML exon 3 has internal alternative splice sites (Breitbart *et al.*, 1987) and that the PML/RAR α isoforms originate from the alternative splicing of different portions of a retained intron.

In summary, *bcr1*, *bcr2* and *bcr3* PML/RAR α junctions differ. Whereas PML/RAR α mRNA junctions are identical within *bcr1* and *bcr3* cases, in *bcr2* they differ from

case to case. In consequence, *bcr1* transcripts would be expected to encode a 105 kDa PML/RAR α protein, *bcr3* a 89 kDa, but the putative proteins of *bcr2* would be in the range 96–105 kDa.

Chromosome 15 heterogeneity and usage of RAR α alternative polyadenylation sites are responsible for the variable length of the PML/RAR α transcripts

PML (LAEP, see Figure 2A) and RAR α (IT, Longo *et al.*, 1990b) DNA probes cohybridized to four different PML/RAR α fusion transcripts of 4.4, 4.0, 3.6 and 3.2 kb in Northern blot experiments of APL RNAs. The 3.6 and the 4.4 kb transcripts comigrated with the 3.8 kb RAR α and the 4.6 kb PML normal transcripts respectively. All nine *bcr1* and two *bcr2* APLs examined expressed the 4.4 and 3.6 kb fusion transcripts, while all 10 *bcr3* APLs examined expressed the 4.0 and 3.2 kb fusion transcripts (data not shown). Two PML/RAR α cDNAs isolated by screening the APL case 22 cDNA library differed in their 3' untranslated regions due to the alternative usage of two RAR α polyadenylation sites [AATAA at positions 2037 or 2888 of the RAR α sequence reported by Giguere *et al.* (1987)]. Since the size of each fusion transcript was that predicted, the variable position of the chromosome 15 breakpoints and the alternative usage of polyadenylation sites must be responsible for the different sizes of the PML/RAR α transcripts.

Identification of heterogeneous PML/RAR α proteins

Representative APL cases were investigated by Western blotting (Figure 5) using a polyclonal antibody (Ab) directed against the RAR α F domain [RP α (F); see Materials and methods]. A prominent, immunoreactive protein of ~110 kDa was seen in one *bcr1* (case 10) and two *bcr2* (cases 13 and 20) APL cases and in COS-1 cells expressing

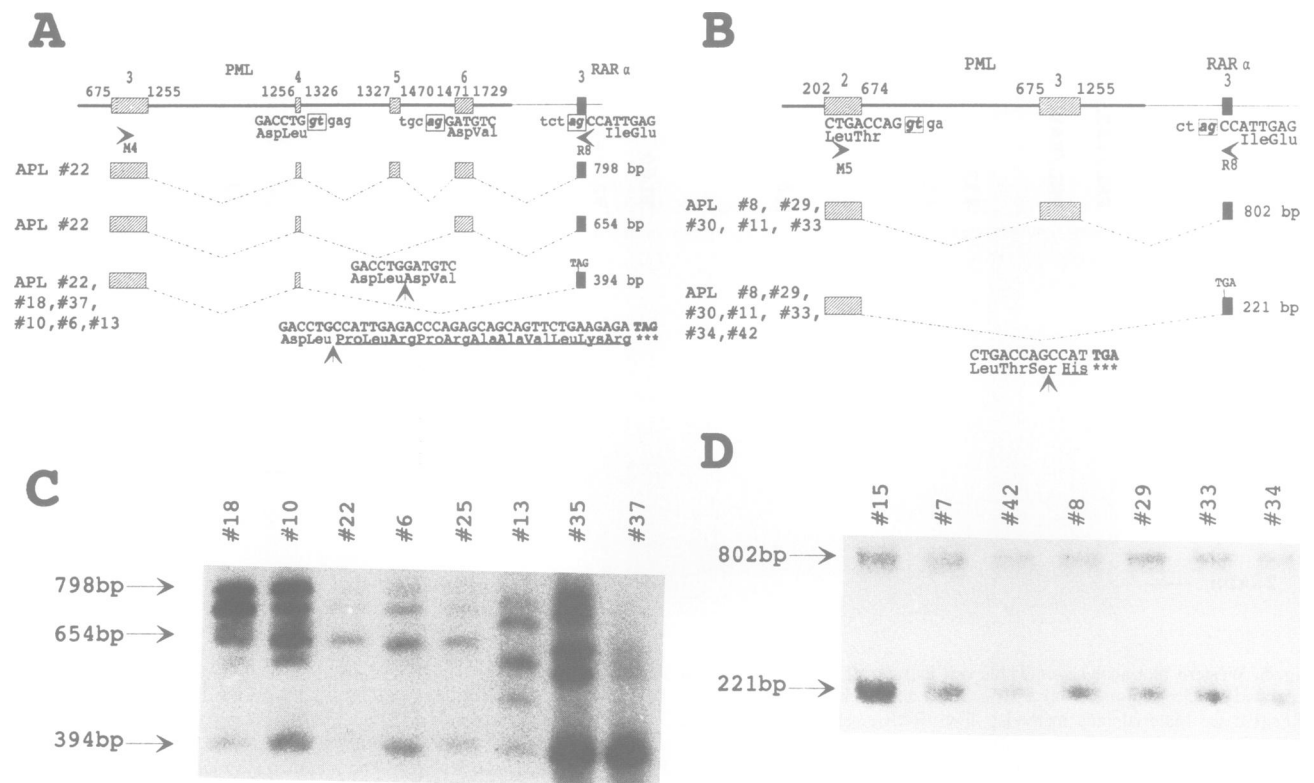


Fig. 6. Alternatively spliced PML/RAR α transcripts. (A and B) A schematic diagram of a representative *bcr1* (A) and *bcr3* (B) PML/RAR α genomic junction is given in the upper section. The position and orientation of the M5, M4 and R8 primers are indicated by arrowheads. Schematic diagrams of the exon assembly predicted from the nucleotide sequences of the 798, 654, 394 (A) and 802, 221 (B) PML/RAR α mRNA PCR amplification products from the indicated APL cases are given below. The nucleotide sequences of the exon/intron boundaries involved in these alternative splicings are given below the upper diagrams. The sequence and predicted proteins of the PML/RAR α mRNA junctions are shown below the broken lines. The junctions are arrowed and junctional non-homologous residues underlined. The in-frame termination codon found immediately 3' to the junction in the 394 bp (A) and the 221 bp (B) PCR products are indicated (***). (C and D) PCR blot of eight representative *bcr1/2* (C) and seven representative *bcr3* (D) APL cases (case numbers are shown above each blot). PCR amplified fragments were hybridized to 20mer oligonucleotides from PML exon 3 (C) and exon 2 (D) (see Materials and methods).

a PML/RAR α *bcr1* cDNA. An ~ 90 kDa protein was detected in three *bcr3* (cases 29, 42 and 8) APLs and in COS-1 cells expressing a *bcr3* PML/RAR α cDNA. None of these proteins was detected in non-APL negative controls such as HL-60 cells and RAR α expressing COS-1 cells (Figure 5). These results suggest that the two immunoreactive proteins of ~ 110 kDa and 90 kDa correspond to *bcr1/bcr2* and *bcr3* PML/RAR α proteins and confirm the predicted heterogeneity. An ~ 48 kDa band was seen in the HL-60 extracts, which corresponds to endogenous RAR α protein. A similar migrating protein was also detected in all but one (APL case 20) of the APLs. The ratio between the PML/RAR α and RAR α band intensities greatly varied among APL cases.

The fact that the molecular weights of the PML/RAR α proteins seen in Western blotting were slightly different from those predicted by the cDNA sequence analysis was probably due to the post-translational modifications (such as phosphorylation) of the RAR α portion of the PML/RAR α protein (M.-P.Gaub, C.Rochette-Egly, Y.Lutz, S.Ali, H.Matthes, I.Scheuer and P.Chambon, in preparation).

Single APL cases express differently spliced PML/RAR α transcripts encoding multiple PML/RAR α isoforms and PML aberrant proteins

bcr1/2 cases were further analysed to determine whether they expressed alternatively spliced PML/RAR α transcripts other than those identified in the *bcr3* APLs. *bcr1/2* RNAs were 1404

analysed by PCR with the M4 and R8 primers, as indicated in Figure 6A. Four major amplification products between ~ 600 and 800 bp and one of ~ 400 bp were variably expressed in the 12 *bcr1/2* cases analysed (see Figure 6C for eight representative cases). A 798 bp and a 654 bp amplification product were isolated from case 22 and sequenced. Whereas PML exons 3–6 were joined to RAR α in the 798 bp fragment of this case, the 654 bp product lacked PML exon 5 (Figure 6A). The other 600–800 bp fragments are presumably derived from the transcripts corresponding to the 798 and 654 bp fragments but have the same alternative splicing within exon 3 as those from *bcr3* APLs. Because the ~ 400 bp PCR fragment was highly expressed in case 37, this case was selected for cloning (Figure 6C). Nucleotide sequencing established that this fragment was 394 bp long and formed by the juxtaposition of PML exon 4 to RAR α exon 3 and the splicing out of PML exons 5 and 6 (Figure 6A). In the *bcr2* case 13 the number of PCR amplification fragments was the same as in the other *bcr1* cases; however, they all migrated slightly faster in the PCR blot (Figure 6C). This was probably due to the fact that, as shown in Figure 4A, only a portion of PML exon 6 sequences joined to the RAR α exon 3.

An additional alternatively spliced PML/RAR α transcript was identified by PCR amplification of *bcr3* cases with primers M5 (from PML exon 2) and R8 (Figure 6B). Two PCR products of 802 and 221 bp were identified in 12 *bcr3* APLs (see Figure 6D for seven representative cases) and

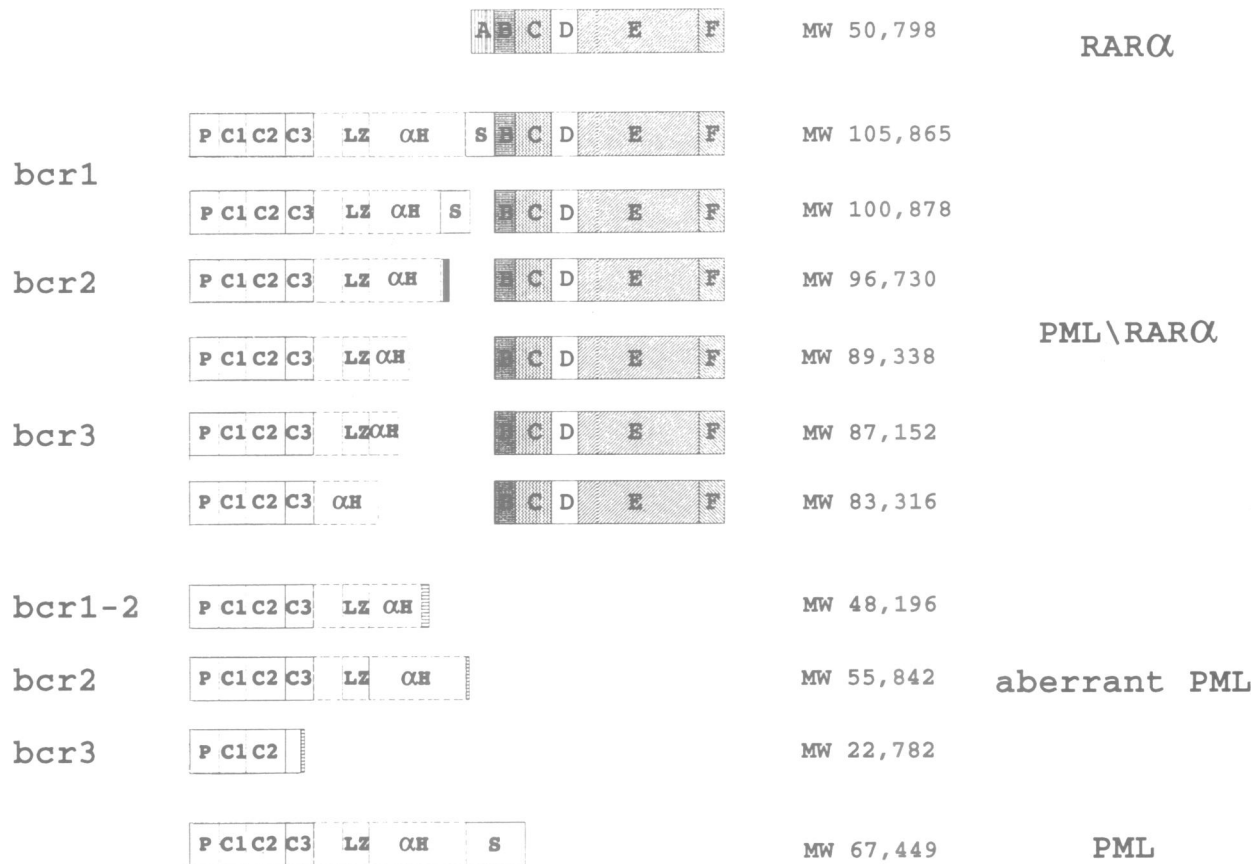


Fig. 7. Modular organization of RAR α , PML/RAR α , aberrant PML and PML proteins. The A–F RAR α and the putative PML domains are illustrated for each putative protein, as indicated. The putative PML domains are designated as in Figure 2. The predicted molecular weight of each putative protein is given on its right. The black box of the *bcr2* PML/RAR α isoform represents junctional non-homologous residues. The hatched boxes of the PML aberrant proteins indicate new C-terminal residues.

isolated from case 8 (Figure 6B and D). While the 802 bp fragment corresponded to the expected PML exons 2–3 RAR α exon 3 joining, the 221 bp fragment resulted from the joining of PML exon 2 to RAR α exon 3.

Surprisingly, two of these newly identified PML/RAR α transcripts would be expected to encode an aberrant PML protein. They are represented by the 394 bp product derived from *bcr1* case 37 and the 221 bp product derived from *bcr3* case 8 (Figure 6A and B). The PML longest ORF terminates 33 and 4 bp beyond the breakpoint site respectively. The finding of PCR amplification fragments of 394 and 221 bp in all cases examined suggests that transcripts encoding aberrant PML proteins are a common feature of APLs. In fact, these transcripts were isolated from additional cases: *bcr1* cases 22, 18, 10 and 6, *bcr2* case 13, and *bcr3* cases 39, 30, 11, 33, 34 and 42.

Modular organization of PML/RAR α isoforms and PML aberrant proteins

Figure 7 is a schematic drawing of all PML/RAR α and aberrant PML isoforms deduced from the PML/RAR α junction sequenced and shows the putative PML and RAR α domains retained in each. If one assumes that the t(15;17) is the crucial event underlying promyelocytic leukaemogenesis, these isoforms must be spontaneous mutants with analogous oncogenic properties. In this case, comparative analysis of these isoforms should allow identification of the regions indispensable for oncogenesis. The PML proline-rich and cysteine-rich domains and the RAR α B–F domains are

common to all PML/RAR α isoforms, and were the only domains present in the sole isoform expressed in APL case 31 (Figure 3D). Therefore, it would seem that they are indispensable and sufficient for promyelocytic oncogenesis. In the same way, the PML proline-rich and the first two clusters (C1; C2) of the PML cysteine-rich motifs appear to be indispensable and sufficient for the biological function of the putative PML aberrant protein.

Discussion

This paper reports the detailed analysis of the molecular architecture of the 15;17 translocation in a large series of APL cases.

The chromosome 17 breakpoint is not distributed randomly within the RAR α locus, but localized within an ~16 kb DNA fragment of the RAR α intron 2. We have mapped the most 5' exon of the human RAR α isoform 2 to this intron (P.P. Pandolfi and P.G. Pelicci, unpublished results), as has previously been done for the mouse RAR α isoform 2 (Leroy *et al.*, 1991). However, the chromosome 17 breakpoints were distributed both 5' and 3' to the RAR α isoform 2 exon 1 and sequences from this exon were never found in any PML/RAR α transcript. In consequence, it would seem that this exon has no influence on the translocation architecture. The position of the chromosome 17 breakpoints presupposes that the chimeric PML/RAR α locus retains the sequences that code for the B–F RAR α domains, while the sequences that code for the A domain remain on 17 to

become 5' to the translocated PML portion in the reciprocal RAR α /PML gene.

The chromosome 15 breakpoint, like that of 17, appears not to be randomly localized within the PML locus. Only three regions of the PML locus are involved in the translocation breakpoints: intron 3 (*bcr3*; 40% of cases), exon 6 (*bcr2*; 20% of cases), intron 6 (*bcr1*; 40% of cases). The heterogeneous PML/RAR α proteins identified by the anti-RAR α Ab provide the first evidence that the predicted fusion proteins actually exist. The PML region retained in all fusion proteins consisted of 342 N-terminal amino acid residues. This region contains three cysteine-rich clusters with striking homology to the DNA binding zinc finger motif of numerous transcription factors (Berg, 1990; Freemont *et al.*, 1991). The coexisting multiple RAR α and putative PML DNA binding domains are probably essential for the function of the chimeric PML/RAR α transcription factor. Instead the PML leucine zipper homologous region (Cohen *et al.*, 1988; Zerial *et al.*, 1989) does not seem to be indispensable. Despite the fact that the leucine zipper homologous region is encoded by sequences proximal to the most 5' *bcr* (*bcr3*), some *bcr3* APLs express mainly PML/RAR α isoforms that exclude a large portion of this region (Figure 3D, case 31). However, even in these cases, a part of the α -helical domain that may still function as a dimerization interface is retained.

Strikingly, an alternatively spliced PML/RAR α transcript that coded for an aberrant PML protein was present in all APL cases analysed. The PML/RAR α junction was composed of PML exon 4 and RAR α exon 3 in the *bcr1* and *bcr2* APL cases, and PML exons 5 and 6 were spliced out; while in the *bcr3* the PML exon 2 and the RAR α exon 3 were juxtaposed and the PML exon 3 spliced out. The level of expression of these transcripts was lower than those encoding PML/RAR α proteins (RNase protection experiments, data not shown). The *bcr1/2* and *bcr3* predicted aberrant PML proteins contained the N-terminal PML portion and shared the first two cysteine-rich clusters, lacked the C-terminal PML residues, but contained 2–11 residues derived from RAR α sequences at the C terminus (Figure 6A and B). The missing segment of the PML aberrant protein is rich in serine and proline. Since it has been proposed that this region is a substrate for serine/threonine protein kinases and/or phosphatases (Kakizuka *et al.*, 1991), its loss could dramatically alter PML function.

The heterogeneity of the PML/RAR α transcript is the result of the variability in the chromosome 15 breakpoint, alternative splicing of the PML portion and alternative usage of two RAR α polyadenylation sites. If it is assumed that we have identified all PML splicing patterns, one should be able to predict the PML/RAR α junction and the resulting protein(s) derived from breakpoints within any PML intron. In this case, breakpoints other than *bcr1/2/3* should generate either the aberrant PML or the PML/RAR α protein. However, only *bcr1/2/3*, and no other breakpoints, would permit the generation of both PML aberrant and PML/RAR α fusion proteins. It therefore seems that only the chromosome 15 breakpoints that allow the formation of both a fusion PML/RAR α and a PML aberrant protein are selected by the leukaemic phenotype; this suggests that the presence of both PML/RAR α and aberrant PML proteins is crucial for the leukaemogenic process.

However, the precise part these two proteins play in leukaemogenesis remains undefined. Since PML/RAR α is

a fusion protein that retains important RAR α and putative PML functional domains, it should have an equal chance of functioning as an abnormal PML protein, an abnormal RAR α protein or both. Therefore, *in vivo*, the abnormal PML/RAR α fusion protein would be expected to interfere with either the endogenous PML or RAR α activation pathways. As RAR α is involved in regulating myeloid differentiation (Collins *et al.*, 1990), it would be logical to suppose that PML/RAR α antagonizes RAR α . This oversimplified explanation, however, ignores the facts that PML/RAR α functions as a RA inducible enhancer factor in most of the promoters tested *in vitro* (de Thé *et al.*, 1991; Kakizuka *et al.*, 1981; Pandolfi *et al.*, 1991) and that APLs respond to RA *in vitro* and *in vivo* (Huang *et al.*, 1988; Castaigne *et al.*, 1990; Chomienne *et al.*, 1990; Lo Coco *et al.*, 1991; Warrel *et al.*, 1991). The finding of an aberrant PML protein in all APL cases examined is evidence that the PML activation pathway is deregulated in APLs. The effects that PML/RAR α and aberrant PML exert on the myeloid differentiation programme now require urgent investigation.

This is the first time a single genetic abnormality, t(15;17), has been demonstrated to generate two potentially oncogenic proteins. Such a dual event could shorten the time required for a target cell to become fully transformed. The picture is further enriched by the finding that the reciprocal RAR α /PML gene is expressed (Kakizuka *et al.*, 1991) and that the same cases expressing PML/RAR α and aberrant PML also expressed a functional RAR α /PML mRNA (Alcalay *et al.*, 1992). The fact that APLs, unlike most other neoplasias, are characterized by a single cytogenetic abnormality (Mitelman, 1988) and lack *ras* and *p53* mutations (L. Longo, P.G. Pelicci and A. Neri, submitted), raises provocative questions.

Materials and methods

Southern and Northern blot analyses

Involved bone marrow was collected from untreated patients during the course of diagnostic procedures. Diagnosis of APL was established in each case by standard clinical and cytological criteria, according to the FAB (French–American–British) recommendations (Bennet *et al.*, 1976). DNA and RNA extraction and Southern and Northern blot analyses were performed according to established procedures (Sambrook *et al.*, 1989).

Isolation of PML/RAR α genomic λ clones from three APL cases and wild type PML genomic λ clones

PML/RAR α λ clones were isolated from genomic libraries constructed by cloning *Mbo*I partially digested DNAs from cases 8, 26 and 28 into the *Xho*I site of the λ -Fix-II vector (Stratagene, CA, USA). PML genomic λ clones were isolated from a commercially available genomic library obtained from human embryo lung fibroblasts (WI38) in the λ -Fix-II vector (Stratagene). Genomic library screening, plaque purification and phage DNA analysis were performed by standard procedures (Sambrook *et al.*, 1989). Restriction enzyme fragments containing the PML/RAR α crossover junctions were subcloned into the plasmid vector pGEM3 (Promega Corporation, WI, USA) and the breakpoint region sequenced. PML cDNA hybridizing restriction enzyme fragments from wild type PML λ phages were subcloned in plasmid vector pGEM3 (Promega) and the exon/intron boundaries sequenced. DNA sequence analysis was performed by the Sanger dideoxy-mediated chain termination method (Sambrook *et al.*, 1989).

Isolation of PML/RAR α mRNA junctions

Single stranded cDNAs were generated from 1 μ g of APL total RNA using a commercial kit (Promega RiboClone cDNA Synthesis System; Promega) and amplified in a standard 40 cycle PCR reaction (Saiki *et al.*, 1988). The denaturing temperature was always 94°C. The annealing temperature varied from 50°C to 60°C and was optimized for each couple of primers. The elongation temperature was fixed at 72°C. The MgCl₂ final concentration varied from 1 to 2 mM. The primers used were: M2, 5'-AGTGTACGCCCTTCTCCATCA-3'; M4, 5'-AGCTGCTGGAGGCTG-

TGGACGCGCGGTACC-3'; M5, 5'-GACTTCTGGTCTTTGAGTG-3' as 5' primers and R8 (5'-CAGAAGCTGCTCTGGGTCTCAAT-3') as the 3' primer. The position of each primer is given in Figures 3, 4 and 6. The PCR blots were hybridized with the following primers: 5'-GACCAACAACATCTTCTGCT-3' (from PML exon 2); 5'-ACGGCAGCTTGCAGGCTCTG-3' (from PML exon 3); 5'-AAGGCCCTTCT-ATGGAGAG-3' (from PML exon 5), according to established procedures (Sambrook *et al.*, 1989). The PCR amplified fragments were cloned into the pCR1000 vector using the Invitrogen TA Cloning System (Invitrogen, CA, USA). T7 and M13 forward primers present in the pCR1000 vector were used for sequencing.

Characterization of RAR α and PML/RAR α proteins by Western blotting

COS-1 cells transfected with the expression vectors for *bcr1* or *bcr3* PML/RAR α and human RAR α -1, and APL blasts were treated as described by Rochette-Egly *et al.* (1992). They were homogenized at 0°C with a glass Dounce B homogenizer in two volumes of buffer (120 mM Tris-HCl, pH 7.8, containing 1 mM EDTA, 0.6 M KCl, 1 mM phenylmethylsulphonyl fluoride, 0.5 mM dithiothreitol) containing a protease inhibitor cocktail (leupeptin, aprotinin, pepstatin, antitrypsin and chymostatin at 0.5 μ g/ml each). After centrifugation, aliquots of the supernatant were fractionated by electrophoresis on a 10% SDS-acrylamide gel and electrotransferred to nitrocellulose sheets. Nitrocellulose sheets were blocked in PBS/3% non-fat powdered milk and then incubated for 2 h at 37°C with the rabbit polyclonal Ab RP α (F) (M.P.Gaub *et al.*, in preparation). After extensive washing the blots were incubated for 90 min with radioiodinated protein A at 25°C, dried and autoradiographed.

Acknowledgements

We are grateful to Dr Fr.Grignani for many helpful discussions, and to Dr G.P.Talamo and L.Venturini for contributions to some experiments. This work was supported by a grant from the AIRC and 'Progetto Finalizzato Oncologia, CNR' to P.G.P. and F.G., and by a 'Biotecnologie e Biostrumentazione' grant.

References

- Alcalay, M. *et al.* (1991) *Proc. Natl. Acad. Sci. USA*, **88**, 1977–1981.
 Alcalay, M. *et al.* (1992) *Proc. Natl. Acad. Sci. USA*, in press.
 Beato, M. (1989) *Cell*, **56**, 335–344.
 Bennet, J.M., Catovski, D., Daniel, M.T., Flandrin, G., Galton, D.A.G., Gralnick, H.R. and Sultan, C. (1976) *Br. J. Haematol.*, **33**, 451–458.
 Berg, J.M. (1990) *J. Biol. Chem.*, **265**, 6513–6516.
 Biondi, A. *et al.* (1991) *Blood*, **77**, 1418–1422.
 Borrow, J., Goddard, A.D., Sheer, D. and Solomon, E. (1990) *Science*, **249**, 1577–1580.
 Brand, N.J., Petkovich, M. and Chambon, P. (1990) *Nucleic Acids Res.*, **18**, 6799–6806.
 Breitbart, R.E., Andreadis, A. and Nadal-Ginard, B. (1987) *Annu. Rev. Biochem.*, **56**, 467–495.
 Breitman, T.R., Selonick, S.E. and Collins, S.J. (1980) *Proc. Natl. Acad. Sci. USA*, **77**, 2936–2940.
 Castaigne, S., Chomienne, C., Daniel, M.T., Ballerini, P., Berger, R., Fenaux, P. and Degos, L. (1990) *Blood*, **76**, 1704–1709.
 Chomienne, C., Ballerini, P., Balitrand, N., Daniel, M.T., Fenaux, P., Castaigne, S. and Degos, L. (1990) *Blood*, **76**, 1710–1717.
 Cohen, D.R. and Curran, T. (1988) *Mol. Cell. Biol.*, **8**, 2063–2069.
 Collins, S.J., Robertson, K.A. and Muller, L. (1990) *Mol. Cell. Biol.*, **10**, 2154–2163.
 de Thé, H., Chomienne, C., Lanotte, M., Degos, L. and Dejean, A. (1990) *Nature*, **347**, 558–561.
 de Thé, H., Lavau, C., Marchio, A., Chomienne, C., Degos, L. and Dejean, A. (1991) *Cell*, **66**, 675–684.
 Evans, R.M. (1988) *Science*, **240**, 889–895.
 Evans, R.M. and Hollenberg, S.M. (1988) *Cell*, **52**, 1–3.
 Freemont, P.S., Hanson, I.M. and Trowsdale, J. (1991) *Cell*, **64**, 483–484.
 Giguere, V., Ong, E.S., Segui, P. and Evans, R.M. (1987) *Nature*, **330**, 624–629.
 Green, S. and Chambon, P. (1988) *Trends Genet.*, **4**, 309–314.
 Huang, M.E., Yu-chen, Y., Shu-rong, C., Jin-ren, C., Jia-Xiang, L., Long-jun, G. and Zhen-yi, W. (1988) *Blood*, **72**, 567–572.
 Jackson, I.J. (1991) *Nucleic Acids Res.*, **19**, 3795–3798.
 Kakizuka, A., Miller, W.H., Jr, Umesono, K., Warrell, R.P., Jr, Frankel, S.R., Murty, V.V.V.S., Dmitrovsky, E. and Evans, R.M. (1991) *Cell*, **66**, 663–674.

- Leroy, P., Krust, A., Zelent, A., Mendelsohn, C., Garnier, J.-M., Kastner, P., Dierich, A. and Chambon, P. (1991) *EMBO J.*, **10**, 59–69.
 Lo Coco, F. *et al.* (1991) *Blood*, **77**, 1657–1659.
 Longo, L. *et al.* (1990a) *Oncogene*, **5**, 1557–1563.
 Longo, L. *et al.* (1990b) *J. Exp. Med.*, **172**, 1571–1575.
 Miller, J., McLachlan, A.D. and Klug, A. (1985) *EMBO J.*, **4**, 1609–1614.
 Mitelman, F. (1988) *Catalog of Chromosome Aberrations in Cancer*. Third edn. Alan R. Liss, Inc., New York.
 Pandolfi, P.P., Grignani, F., Alcalay, M., Mencarelli, A., Biondi, A., Lo Coco, F., Grignani, F. and Pelicci, P.G. (1991) *Oncogene*, **6**, 1285–1292.
 Petkovich, M., Brand, N.J., Krust, A. and Chambon, P. (1987) *Nature*, **330**, 444–450.
 Rochette-Egly, C., Lutz, Y., Saunders, M., Gaub, M.-P. and Chambon, P. (1992) *J. Cell Biol.*, **92**, in press.
 Saiki, R.K., Gelfand, D.H., Stoffel, S., Scharf, S.J., Higuchi, R., Horn, G.T., Mullis, K.B. and Erlich, H.A. (1988) *Science*, **239**, 487–491.
 Sambrook, J., Fritsch, E.F. and Maniatis, T. (1989) *Molecular Cloning. A Laboratory Manual*. Cold Spring Harbor Laboratory Press, Cold Spring Harbor, NY.
 Sawyers, C.L., Denny, C.T. and Witte, O.N. (1991) *Cell*, **64**, 337–350.
 Warrel, R.P., Jr *et al.* (1991) *N. Engl. J. Med.*, **324**, 1385–1393.
 Zerial, M., Toschi, L., Ryseck, R.P., Schuermann, M., Muller, R. and Bravo, R. (1989) *EMBO J.*, **8**, 805–813.

Received on November 22, 1991

Note added in proof

The sequence data reported in this paper have been deposited in the EMBL Data Library under the accession numbers X63631 and X63647.